Advances in Environmental Technology 2 (2018) 107-117

Advances in Environmental Technology

journal homepage: http://aet.irost.ir

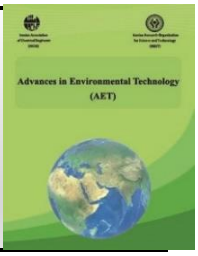

Xylene removal from dilute solution by palm kernel activated charcoal: Kinetics and equilibrium analysis

Rahman Pazira, Asghar Lashanizadegan[1]*, Hakimeh Sharififard, Parviz Darvishi

Chemical Engineering Department, Yasouj University, Yasouj, Iran

ARTICLE INFO

Article history:
Received 22 June 2018
Received in revised form
21 October 2018
Accepted 24 October 2018

Keywords:
Activated charcoal
Palm kernel waste
Xylene
Adsorption

ABSTRACT

Xylene is an aromatic hydrocarbon and a highly toxic compound. Therefore, it is essential to remove this component from wastewater before discharging it into the environment. In this research, palm kernel biomass was activated chemically by H_3PO_4 and the resulting synthesized activated charcoal was applied to separate xylene from aqueous media. The prepared activated charcoal was characterized using FTIR, BET, SEM, pH_{zpc} measurement, and Boehm analysis methods. The characterization tests indicated that the produced activated carbon had an acidic character with various functional groups and a micropores structure. The values of the external mass transfer coefficients ranged from 1.87×10^{-5} to 1.90×10^{-5}. By increasing the temperature, the pore and surface diffusion coefficients increased from 1.15×10^{-9} to 1.91×10^{-9} and 6.98×10^{-16} to 7.58×10^{-16}, respectively. The sensitivity analysis indicated that pore diffusion and film diffusion were the main mass transfer parameters. The equilibrium analysis also revealed that the multilayer model with saturation could well describe the data. The number of adsorbate ions for one site, the number of adsorption layers, the density of the receptor site, and the energy of the adsorption at layers were determined using statistical physics modelling. The maximum capacity of the prepared activated charcoal at the experimental condition for xylene adsorption was 23.48 mg/g .

1. Introduction

Volatile organic compounds (VOCs) are liquid or solid materials that evaporate rapidly and contain components such as charcoal, hydrogen, nitrogen or sulfur. These compounds have the highest frequency and diversity of diffusion after the suspended particles. VOCs are produced and released from various sources and may have a detrimental effect on human health and performance. Xylene is one of the VOCs that are widely employed in numerous industries: rubber, paint, adhesives, plasters, lubricants and inks, plating, leather and paper, detergents and cleaners, and various types of fuels. Also, xylene isomers are added to gasoline as a supplement. Xylene isomers are used as industrial solvents and take part in many synthetic reactions as intermediates. Xylene is any one of three isomers of dimethylbenzene ($(CH_3)_2C_6H_4$) or a combination thereof. The chemical structure of dimethylbenzene isomers are presented in Figure 1. Xylene enters the body through various routes causing problems such as cancer, nervous system disorders, dizziness, nausea, drowsiness, coma, liver, and kidney diseases [1-3]. There are several techniques for separating xylene from industrial water and wastewater, including biological treatment, catalytic and thermal oxidation, adsorption, and membrane methods [3-7]. Recently, the adsorption process is highly regarded as an alternative method in comparison with the

---

*Corresponding author. Tel: +98-7431005067
E-mail address: : lashani@yu.ac.ir
DOI: 10.22104/AET.2018.2989.1145

other separation techniques. This process provides many advantages including easy operation and control, high potential and efficiency, and low costs to bring about the separation more effectively [8-11].

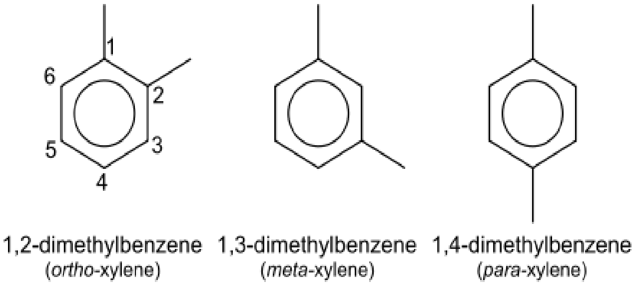

Fig. 1. Chemical structure of xylene isomers

From a process standpoint, the selected adsorbent is an important parameter affecting process efficiency. Among the available industrial adsorbents, activated charcoal has attracted increased attention due to its unique porous structure and high chemical and mechanical resistance [12-14]. Due to the high cost of commercial charcoal, researchers are searching for cheaper, affordable and accessible materials to produce activated charcoal. Agricultural and industrial wastes may be considered as suitable raw materials to produce the desired activated charcoal [15]. The synthesis of activated charcoal from these materials can be performed via chemical and physical processes. The combination of physical conversion by physical activation and chemical changes via chemical activation can pave the way to produce activated charcoal with the desired adsorption properties. In this regard, it should be implied that the choice of a suitable activation agent is very important for obtaining the desire activated charcoal characteristics. Agricultural wastes including the stones, shells, and seeds of various fruits, sewage slags and biomass are being applied to produce activated charcoal [15-22]. One of the abundant agricultural products in IRAN are date palm, which are widely cultivated across the southern part the country. Iran is the world's second-largest producer of date palm. Therefore, the large amounts of agricultural residues generated in the form of palm kernels could be used as raw materials for producing activated charcoal. This research aims to investigate the removal of xylene from the dilute solution in the batch process by using the activated charcoal produced from palm kernel biomass. To explore the mechanism of adsorption, as well as the effectiveness of the separation, the kinetics and equilibrium data are analysed via various models.

2.Materials and methods

2.1.Materials

The palm kernel biomass was gathered from palm trees in Bushehr, Iran. The kernel waste was washed and dried for 3 days in the open air. The biomass was ground and screened to obtain the specific particle size (Mesh: 30-40). Pure H_3PO_4, HCl (37 %), NaOH, and isomeric xylene solution with 99.90 % purity were supplied from the Merck Company.

2.2.Production of activated charcoal

A chemical activating method was adopted to synthesize the activated charcoal. Chemical activation was performed in the following manner. The dried biomass was immersed in a H_3PO_4 solution (85 % v/v). The ratio of chemical agent mass to raw material mass was 6.0. The biomass impregnated with phosphoric acid was filtered and dried at 110 ºC for one day. The raw material impregnated with chemical agents was carbonized according to the method presented in our previous works [15-16]. The carbonization temperature and time were 400 °C and 100 min, respectively.

The production yield of the synthesize process was calculated as:

$$\textit{production yield}=\frac{\textit{Activated charcoal mass after washing step}}{\textit{Raw material mass}} \qquad (1)$$

2.3.Activated charcoal characterization

In order to measure the apparent density of the adsorbent, the dry charcoal was poured into a certain volume in a dry and well-weighed cylinder. The mass of the cylinder with the adsorbent was measured and used to calculate the apparent density [10]. In order to measure the ash content of the prepared activated charcoal, a standard method (EN 14775:2010) [23] was applied. 0.1 g of dried activated charcoal was placed into a weighed and dried crucible. This crucible was put in a furnace at 550 ºC for 1 h. After cooling, the mass of the residual matter in the crucible was measured and used to calculate the ash percentage according to the following equation:

$$\text{Ash}(\%) = \frac{\text{The mass of remaining material (g)}}{\text{The mass of dried adsorbent (g)}} \qquad (2)$$

The moisture content of the prepared activated charcoal was determined according to a standard test method (ASTM D 2867-91) [24].The amount of surface functional groups onto activated charcoal surface was determined according to the Boehm method. In this method, 0.1 g dried charcoal was added to some glass flasks containing HCl, NaOH, $NaHCO_3$ and Na_2CO_3 solutions (0.1 N, 25 mL). The flasks were shaken for 48 h at 25 ºC. After filtration, the remaining solutions were titrated with NaOH and HCl solutions (0.1 N). The obtained data from titration was applied to estimate the amount of surface functional groups [25-26]. The specific surface area of the activated charcoal was measured according to the adsorption and desorption data of N_2 at 77 K by applying the BET method [27]. The chemistry of the activated charcoal surface was analysed via the FTIR method. The morphology of the adsorbent surface was detected by applying a scanning electron microscopy equipped with an EDS analyzer (SEM–EDS; Tescan).

The pH_{ZPC} of adsorbent was measured according to the following procedure: 0.1 g of dried material was put in some glass flasks containing NaCl solution (0.1 N). The initial pH of these solutions was adjusted in the range of 1-12. After shaking them for 1 day, the solutions were filtered and the pHs of the filtrates were measured. The point where the pH of the solution does not change after one day of contact with the adsorbent is expressed as pH_{ZPC} [10]

2.4.Batch adsorption experiments

The influence of some separation parameters namely initial xylene concentration, contact time, and temperatures were evaluated in the batch operation. The impact of contact time on the ability of activated charcoal to remove xylene was studied in the following manner: 0.05 g of activated charcoal was added to a glass flask containing xylene solution (volume = 50 mL, initial concentrations:= 25 mg/L and pH = 6). The flask was shaken for the desired time (5-360 min) at 25 ºC, 35 ºC, and 45 ºC. After filtration, the concentration of xylene that remained in the filtrate was detected by gas chromatography (GC) (Varian-3800, CP-WAX-52CB) and applied to calculate the amount of xylene adsorbed onto the charcoal surface. The equilibrium state of the xylene–activated charcoal system was analysed as follows: 0.05 g of activated charcoal was poured into glass containers containing xylene solution (50 mL) with the desired initial concentration and pH (5 - 25 mg/L, pH = 6). After one day of shaking, filtration was carried out and the filtrate was analysed using GC to detect the remaining xylene concentration. The equilibrium experiments were done at 25 ºC, 35 ºC, and 45 ºC.

2.5. Theory

2.5.1. Determination of mass transfer parameters

Designing an optimal industrial adsorption process to study the influence of the process parameters requires a large number of experiments on a pilot plant scale. Due to the difficulty in performing the experiments, as well as their time-consuming and costly nature, it is desirable to develop a mathematical model to predict the adsorption process.

Listed below are three important mass transfer steps for the adsorption of a component from a liquid phase onto the adsorbent surface:

a) External diffusion (film resistance): In this stage, the molecules or ions of the adsorbate in the bulk solution reach the absorbent surface and pass across the liquid film that is surrounding the adsorbent particle. One of the important mass transfer parameters at this stage is the external mass transfer coefficient (k_f m/s), which expresses the transfer rate of ions or molecules from the liquid film.

b) Internal diffusion: Here, the adsorbate ions or molecules on the adsorbent surface penetrate into the adsorbent structure to fully adsorb all internal adsorbing sites. Internal penetration (diffusion) involves pore and surface diffusion. Pore diffusion is the molecular diffusion (Knudsen diffusion) of the adsorbing ions or molecules in the pores filled with liquid. Pore diffusion occurs mainly in the macro and mesopores. Surface diffusion is the motion of ions or molecules of the adsorbate onto the surface and pore walls of the adsorbent. Surface diffusion is the dominant mechanism in the adsorbent with high porosity and surface area with micropores. Often the pore and surface diffusion of the adsorbate ions or molecules act in parallel. The rate of the internal diffusion step is independent of the hydrodynamic properties of the system. It is dependent on the structure and size of the adsorbent pores. Fick's law is applied to describe the transfer of ions or molecules of the adsorbate in the pore that is filled with liquid, Equation (3), and the motion of the adsorbate ions or molecules onto the surface and pore wall of the adsorbent, Equation (4):

$$J = -D_P \frac{dC_p}{dr} \tag{3}$$

$$J = -D_s \rho_p \frac{dq}{dr} \tag{4}$$

where r is the radial direction for the spherical adsorbent particle, C_p (mg/L) represents the concentration of adsorbate in the solution in the pores of the adsorbent, and q (mg/g) denotes the amount of adsorbate attracted onto the adsorbent surface. D_s (m^2/s) and D_p (m^2/s) stand for the surface and pore diffusion coefficients, respectively. The schematic diagram of the external and internal diffusion steps are shown in Figure 2 [28].

c) The adsorption of ions or molecules on the adsorption sites (functional groups) in the pore wall or adsorbent surface: The adsorption process at this stage can take place as a chemical or/and physical one.

To estimate the mass transfer coefficients including pore diffusion, surface diffusion and external mass transfer coefficients, a mathematical model is needed and can be described as follows. Some assumptions need to be considered here: 1) Adsorbent particles have a spherical geometry; 2) The temperature variation in the adsorption process is negligible; 3) The adsorption of xylene molecules onto the adsorbent surface and pore wall (step 3) is very rapid; and 4) The diffusion of the adsorbate ions into adsorbent particle occurs in a radial direction [29]. The amount of xylene transferred from the bulk liquid to the surface of the adsorbent at each time (dC_b/dt) can be calculated as follows:

$$\frac{dC_b}{dt} = -\frac{3m}{V(4\pi {R_p}^2)\rho_p}(4\pi {R_p}^2)k_f(C_b - C_p|_{r=R_p}) \tag{5}$$

In this equation, C_b (mg/L) represents the concentration of adsorbate in the bulk solution, k_f (m/s) shows the film mass transfer coefficient, and R_p (m) represents the average radius of activated charcoal particles. V and m denote the volume of adsorbate solution and the mass of adsorbent, respectively. The density of the adsorbent particle is presented by ρ_p (Kg m^{-3}). The mathematical equation for describing the adsorption of adsorbate molecules or ions onto the adsorbent surface via pore and surface diffusion and mass transfer equilibrium between the adsorbed phase and the liquid in pores can be shown as follows:

$$\frac{dC_p}{dt}\left[\varepsilon_p + \left(1-\varepsilon_p\right)\frac{dq}{dC_p}\right] = \frac{1}{r^2}\frac{\partial}{\partial r}\left(D_p\varepsilon_p r^2\frac{\partial C_p}{\partial r}\right) + \frac{\rho_p}{r^2}\frac{\partial}{\partial r}\left(D_s\left(1-\varepsilon_p\right)r^2\frac{\partial q}{\partial r}\right) \qquad (6)$$

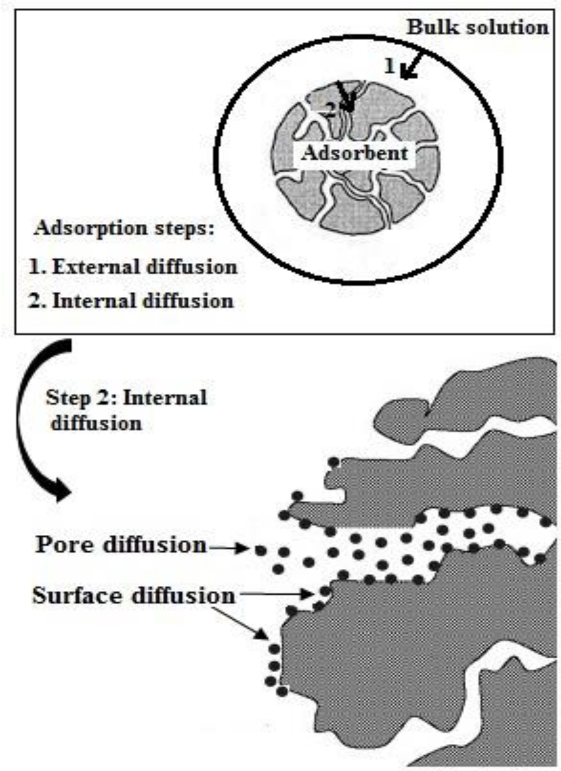

Fig. 2. Schematic of diffusion steps for adsorption of solute from bulk solution.

where ε_p represents the adsorbent particle porosity. The q and C_p parameters are related using the isotherm equation.The initial and boundary conditions are as follows:

$$@t = 0,\ \ C_p(r, t = 0) = 0,\ \ q(r, t = 0) = 0,\ \ C_{b0} = 0 \qquad (7)$$

$$@r = 0 \qquad \frac{dC_p(r = 0, t)}{dr} = 0 \qquad (8)$$

$$@r = R_p \qquad D_p\varepsilon_p\frac{\partial C_p}{\partial r}\bigg|_{r=R_p} + \rho_p D_s\left(1-\varepsilon_p\right)\frac{\partial q}{\partial r}\bigg|_{r=R_p} = k_f\left(C_b - C_p\big|_{r=R_p}\right) \qquad (9)$$

The above PDE equations can be solved using numerical methods such as the finite difference method in order to find C_b at each time (t). The quantitative expression of the function in this program was the root mean square (RMS) [29].

$$RMS = 100 \times \sqrt{\frac{1}{n}\sum_{i=1}^{n}\left(1-\frac{C_b|_{cal,i}}{C_b|_{exp,i}}\right)^2} \qquad (10)$$

2.5.2. The adsorption isotherms for statistical physical modelling

There are several important subjects in the adsorption process that can be used to find the parameters to obtain the number of adsorbate ions or molecules that are adsorbed onto one adsorption site, the number of the receiver adsorption site, and the number of formed adsorption layer. In order to identify these parameters, it is necessary to evaluate the microscopic characteristics of the adsorption process. Sellaoui et al. stated that the microscopic characteristics of the adsorption process can be described using statistical physical modelling [30]. Different equilibrium isotherms have been proposed to investigate the microscopic analysis of the adsorption process: Langmuir, Hill, double layer, and multilayer with saturation. The Langmuir isotherm model is an empirical model and assumes that one adsorption layer is formed in the adsorption process. The mathematical description of this model is as follows:

$$q = \frac{q_{max}K_L C_e}{1+K_L C_e} \qquad (11)$$

where q ((mg/L) and C_e (mg/L) are the quantity of adsorbed components onto the adsorbent surface and the adsorbate concentration remaining in the solution after the adsorption process, respectively. K_L (L/g) is the constant and qmax (mg/L) is the amount of adsorbed components when the adsorbent surface is saturated (monolayer adsorption capacity). This model does not describe the other information, for example, the number of adsorbed ions or molecules onto one adsorption site and the number of the receiver adsorption sites onto the adsorbent surface. For this reason, the model **was** modified and becomes the Hill model. In this modified model, it is assumed that an adsorption layer is formed onto the adsorbent surface and the number of molecules or ions adsorbed in each pore is different. It is possible to determine the number of adsorbed ions or molecules onto one adsorption site by using this isotherm model. The mathematical relationship of the Hill model is as follows:

$$q = \frac{Q_0}{1+\left(\frac{C_{1/2}}{C_e}\right)^n} \qquad (12)$$

This model has 3 adjustable parameters: the amount of adsorbed components on the adsorbent surface in monolayer form (Q_0 mg g^{-1}), the concentration of adsorbate at the half-saturation state of the adsorbent surface ($c_{1/2}$ mg L^{-1}), and the number of adsorbed ions or molecules onto one adsorption site (n). However, it should be noted that the number of formed adsorption layers cannot be determined with this model. Therefore, two isotherm models were applied: the double layer isotherm with two adsorption energies and the multilayer isotherm with saturation. In the double layer model, it is assumed that the adsorption process takes place at two adsorption layers. Also, it is assumed that the adsorption energies of these two adsorption layers aredifferent, where ε_1 and ε_2 (kJ/mol) apply to the first and the second adsorption layers, respectively. The energy of the first adsorption layer is higher than that of the second layer [30]. The double layer model is as follows:

$$q = nN_m \frac{\left(\frac{C_e}{c_1}\right)^2 + 2\left(\frac{C_e}{c_2}\right)^{2n}}{1+\left(\frac{C_e}{c_1}\right)^n + \left(\frac{C_e}{c_2}\right)^{2n}} \tag{13}$$

In this equation, N_m represents the number of receiver adsorption sites onto the adsorbent surface. The parameters c_1 and c_2 are the adsorbate concentration at the half-saturation state for the adsorption layers formed onto the adsorbent surface. Equation (14) presents the multilayer model with saturation (MLM-S).

In the MLM-S model, it is assumed that the adsorbate molecules or ions in the first adsorption layer are adsorbed onto the adsorbent surface by ε_1 energy and the molecules or ions in the other layers are adsorbed by ε_2 energy. In this isotherm model, (N+1) represents the number of formed adsorption layers onto the adsorbent surface. The c_1 and c_2 parameters can be used to determine the adsorption energy per mole of adsorbate for each adsorption layer as follows [30-31].

$$q = nN_m \frac{F_1 + F_2 + F_3 + F_4}{G} ;$$

$$F_1 = -\frac{2\left(\frac{C_e}{c_1}\right)^{2n}}{\left(1-\left(\frac{C_e}{c_1}\right)^n\right)} + \frac{\left(\frac{C_e}{c_1}\right)^n \left(1-\left(\frac{C_e}{c_1}\right)^{2n}\right)}{\left(1-\left(\frac{C_e}{c_1}\right)^n\right)^2};$$

$$F_2 = \frac{2\left(\frac{C_e}{c_1}\right)^{2n}\left(\frac{C_e}{c_2}\right)^n \left(1-\left(\frac{C_e}{c_2}\right)^{nN_m}\right)}{\left(1-\left(\frac{C_e}{c_2}\right)^n\right)}; \tag{14}$$

$$F_3 = -\frac{\left(\frac{C_e}{c_1}\right)^n \left(\frac{C_e}{c_2}\right)^{2n} \left(\frac{C_e}{c_2}\right)^{nN} N}{\left(1-\left(\frac{C_e}{c_2}\right)^n\right)};$$

$$F_4 = \frac{\left(\frac{C_e}{c_1}\right)^n \left(\frac{C_e}{c_2}\right)^{2n} \left(1-\left(\frac{C_e}{c_2}\right)^{nN}\right)}{\left(1-\left(\frac{C_e}{c_2}\right)^n\right)^2};$$

$$G = \frac{\left(1-\left(\frac{C_e}{c_1}\right)^{2n}\right)}{\left(1-\left(\frac{C_e}{c_1}\right)^n\right)} + \frac{\left(\frac{C_e}{c_1}\right)^n \left(\frac{C_e}{c_2}\right)^n \left(1-\left(\frac{C_e}{c_2}\right)^{nN}\right)}{\left(1-\left(\frac{C_e}{c_2}\right)^n\right)}$$

$$\varepsilon_1 = -k_B T ln\left(\frac{c_1}{C_s}\right) \tag{15}$$

$$\varepsilon_2 = -k_B T ln\left(\frac{c_1}{C_s}\right) \tag{16}$$

C_s (mg/g) is the solubility of the adsorbed molecules or ions in water. This work uses the solubility data reported by Coquelet et al. [32]. The ε_1 represents the energy for the adsorbate-adsorbent interactions and ε_2 represents the energy for the adsorbate-adsorbate interactions. In these isotherm models, n displays the number of adsorbed molecules or ions onto one adsorption site. This parameter indicates the geometry of the adsorbate molecules or ions onto the surface of the adsorbent. Also, n can be used to estimate the degree of aggregation of adsorbate molecules or ions [30]. When n <1, it means that one molecule or ion of adsorbate is shared onto two and/or more adsorption sites. In this case, the geometry of adsorbate onto the adsorbent surface is parallel and the adsorption process is a multi-adsorption site (anchorage) process. In this case, it can be said that the adsorbate molecules or ions are adsorbed onto both sides of the pore walls [33]. When n >1, it means that two or more molecules or ions of adsorbate are adsorbed onto one adsorption site and the geometry of the adsorbate ions/molecules onto the surface of adsorbent is inclined resulting in the aggregation of adsorbate molecules or ions. Therefore, the adsorption process is a multi-adsorbate molecule process. All the parameters of these statistical physical models were determined by minimizing Marquardt's percent standard deviation (MPSD) equation via MATLAB 8.4.0. This equation was used to evaluate the accuracy of fitting these isotherm models with the experimental results. According to the obtained results, the regression coefficient is calculated for all equilibrium models. The MPSD equation is calculated as [10]:

$$MPSD = 100 \times \sqrt{\frac{1}{n_m - n_p}} \times \sqrt{\left(\frac{\left(\sum_{i=1}^{N} q_{e,i,exp}\right) - \left(\sum_{i=1}^{N} q_{e,i,cal}\right)}{\sum_{i=1}^{N} q_{e,i,exp}}\right)^2} \tag{17}$$

3. Results and discussion

3.1. Characterization of activated charcoal

Table 1 displays the production yield, moisture percentage, pH_{ZPC}, ash percentage, bulk density, quantity of acidic and basic functional groups, specific surface area (BET), total volume of pores, and average pore diameter for the produced activated charcoal. The value of pH_{ZPC} and the results of Boehm titration indicate that the prepared charcoal has an acidic character. The result of the FTIR analysis for the prepared activated charcoal is presented in Figure 3. The peak at 3420 cm^{-1} indicates the –OH group stretching that presents in the activated material structure. The peak on 2360 cm^{-1} shows the P-H bonds of phosphoric acid. The peaks at 1650 and 1570 cm^{-1} represent the C=O bond stretching in carboxylic acid, ketones, and aldehyde and the vibration of the C=C bond, respectively. The vibrations of C-O in phenyl and acyl are detected by the observed peaks at 1380 and 1260 cm^{-1}. The peak at 1420 cm^{-1} represents the vibration of the C-O-H in carboxylic acid. The FTIR results show that the synthesized activated charcoal has different functional groups that act as accessible adsorption sites onto the surface of activated charcoal and increase the adsorption capacity of the prepared charcoal [15-16]. Figure 4 presents the morphologies of the activated charcoal surface. This figure indicates that activation with H_3PO_4 causes porosity on the charcoal surface. The results of the BET analysis confirm this. The mechanism of porosity development by acidic agents such as H_3PO_4 can be explained in the following manner. In the activation process with phosphoric acid, the molecules of the phosphoric acid are placed between the chains of cellulose and increase the volume by separating the chains. Also, the phosphate ester bonds are formed between the chains of cellulose via these molecules; these bonds are the basic reason for increasing the volume of carbon. The expansion of the volume can be increased by the creation and incorporation of polyphosphates within the structure of carbon via ester bonds with chains of cellulose. This expansion is the basic reason for developing the specific surface area and porosity of the prepared charcoal [34-35].

Table 1. Chemical-physical properties of prepared activated charcoal

		Activated charcoal
Yield (%)		53.17
Moisture (%)		1.62
Bulk density (g/cm)		0.272
Ash content (%)		5.51
pH_{ZPC}		3.00
Surface functional groups (mequiv/g)	Basic	1.730
	Carboxyl	3.182
	Phenolic	0.050
	Lactonic	0.298
BET surface area (m^2/g)		476.43
Average pore diameter (Å)		32.40
Total pore volume (cm^3/g)		0.401

The mechanism of activating with phosphoric acid is as follows: the phosphoric acid usually starts to act and react with the raw material at the early stages of the carbonization process with low temperature. At this reaction, the phosphate ester bonds form between the lignocellulose chains, and these bonds create a layer that protects the inner surface of pores. Therefore, a rigid matrix is formed by these phosphate and polyphosphate ester bonds. This matrix restrains the excessive burning of raw material and consequently leads to a high yield [36].

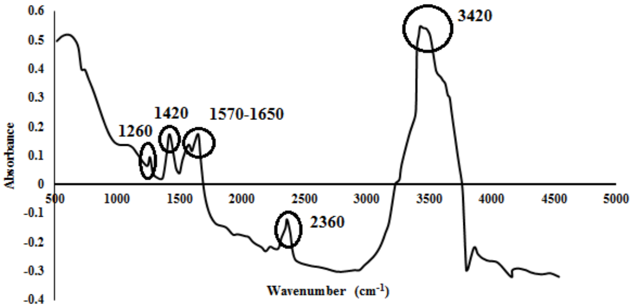

Fig. 3. FTIR spectra of prepare activated charcoal.

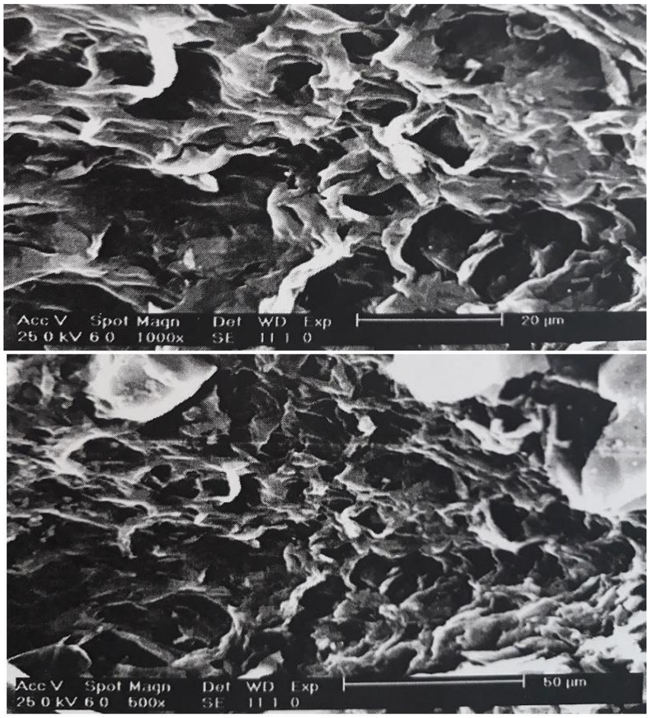

Fig. 4. SEM micrographs of activated charcoal

3.2.Removal of xylene in a batch adsorption process

3.2.1. Kinetics analysis

Figure 5 presents the kinetics data obtained at different temperatures. Also, the calculated data using the presented mathematical model is presented in this figure. A comparison of the experimental data with the calculated data shows that the presented mathematical model has a good ability to predict the behavior of the absorption system. The calculated mass transfer parameters at various temperatures are shown in Table 2.

The data in Table 2 indicates that the magnitude of the external mass transfer, surface and pore diffusion coefficients are in the order of 10^{-5}, 10^{-9}, and 10^{-16}, respectively. The film mass transfer parameter is the hydrodynamic parameter that depends on the hydrodynamic condition of the system (agitation rate); therefore, its values for various temperatures with the same hydrodynamic condition are the same. However, pore and surface diffusion coefficients depend on the chemistry of the adsorbent surface, porosity properties of the adsorbent, the chemistry, and the movement rate of the adsorbate. By raising the temperature, both the energy of the xylene molecules and its penetration rate in the pores increases. Also, its motion onto the surface of activated charcoal increases. As a result, the amount of xylene adsorption increases which implies an increase of the pore and surface diffusion coefficients. The sensitivity analysis is performed to determine the significance and effect of each mass transfer parameter. To conduct this analysis, the adsorption process is simulated at 25 °C with various values of mass transfer parameters and the results are presented at Figure 6.

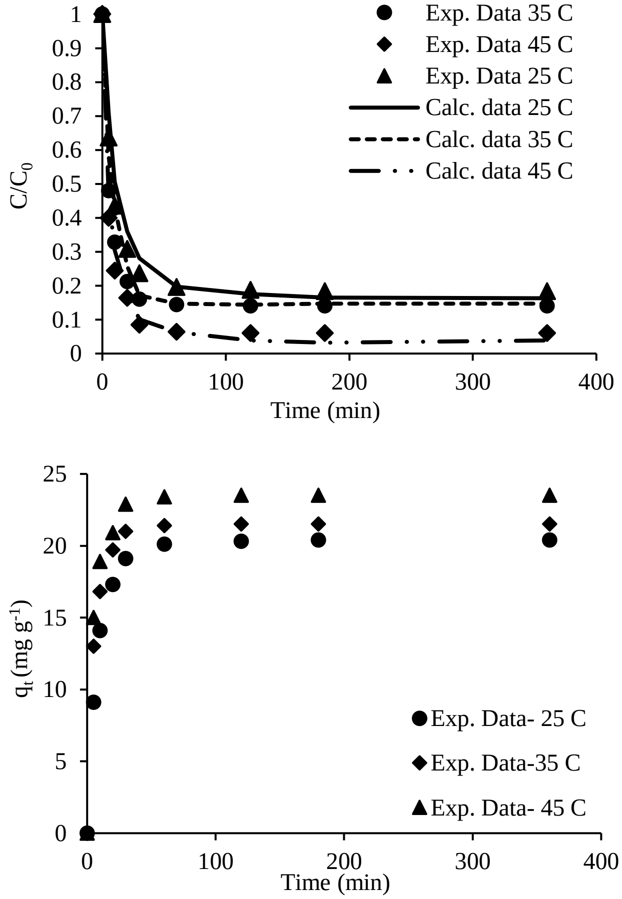

Fig. 5. Influence of contact time on xylene removal ability at various temperatures (dots: experiments result; solid lines: calculated data)

Table 2. The values of RMS and mass transfer parameters for xylene removal using activated charcoal

Parameter	**25 °C**	**35 °C**	**45 °C**
k_f (m/s)	1.87×10^{-5}	1.88×10^{-5}	1.90×10^{-5}
D_p (m^2 /s)	1.15×10^{-9}	1.70×10^{-9}	1.91×10^{-9}
D_s (m^2 /s)	6.98×10^{-16}	7.16×10^{-16}	7.58×10^{-16}
RMS	6.441	5.914	6.183

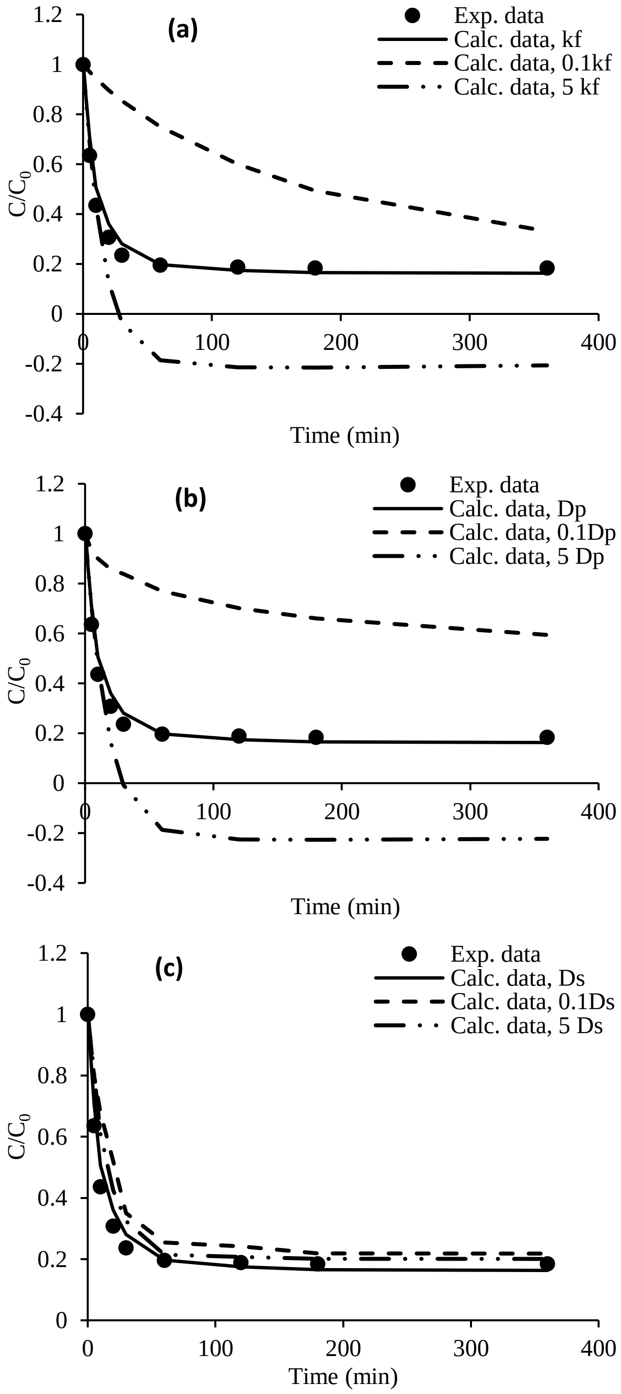

Fig. 6. Results of sensitivity analysis for xylene removal using activated charcoal: (a): k_f, (b): D_p, (c): D_s

The results indicate that the k_f and D_p coefficients are the effective parameters because the curves plotted in the various values of these parameters exhibit very different courses (or trends). However, the surface diffusion coefficient is an unimportant parameter. In general, it can be said that porosity and pore size significantly influence the adsorption of xylene with activated charcoal, and it can be implied that physical absorption is the dominant aspect in this process.

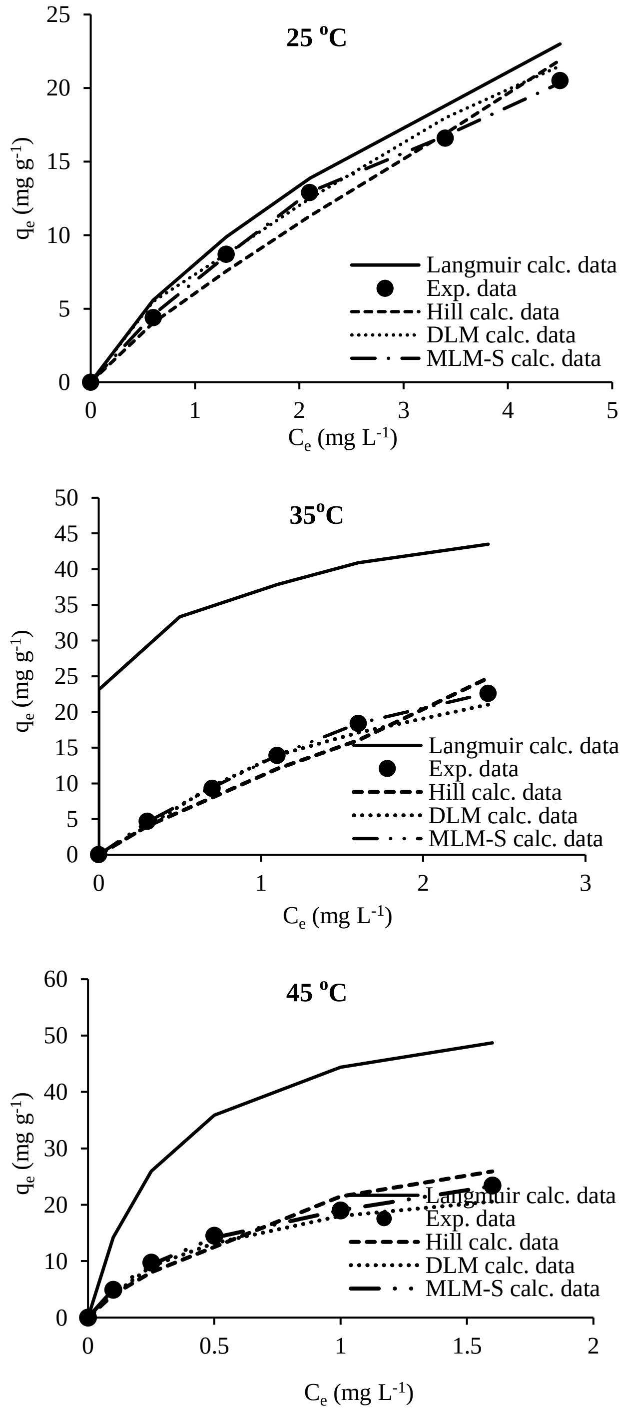

Fig. 7. Adsorption isotherms of xylene removal using prepared activated charcoal

3.2.2. Equilibrium analysis

The equilibrium data for xylene adsorption onto activated charcoal was analyzed using the Langmuir, Hill, double layer, and multilayer with saturation isotherm models. Figure 7 presents the experimental and calculated data using these statistical models. The parameters and R^2 values for these statistical physical isotherms are shown in Table 3. The R^2 values show that the equilibrium adsorption of xylene onto activated charcoal can be described well with the multilayer with saturation isotherm model. Also, the data presented in Figure 7 indicate that the multilayer model with saturation demonstrate well the equilibrium manner for xylene adsorption onto activated charcoal. The statistical physical modeling results show that the number of adsorbed molecules of xylene onto the activated charcoal (n) is lower than one; this implies that the geometry of the xylene molecules adsorbed onto the adsorbent surface is parallel so that the xylene molecules are adsorbed onto both sides of the pore walls. In general, *n* and N_m depend on both the physico-chemical properties of the adsorbate ions and the adsorbent surface [37]. The prepared activated charcoal has different kinds of surface functional groups (carboxylic, hydroxyl, and carbonyl groups) and a high potential for xylene adsorption via physico-chemical interactions; therefore, the number of receiver adsorption sites for adsorption of xylene is high.

Table 3 indicates that the total number of adsorption formed layers (1+N) are greater than one. This means that the xylene adsorption process is multilayer. It can be suggested that xylene is probably adsorbed on the activated charcoal surface via a physical adsorption process. This result is validated by kinetics analysis. The adsorption energies per mole of xylene molecules adsorbed onto the adsorbent surface are shown in Table 4. The values of energies are positive and this indicates that the adsorption process of xylene onto this adsorbent is endothermic. At all temperatures, the adsorption energy of the first layer is higher than that of the second layer. This suggests that the adsorbate molecule-surface functional group interaction is stronger than the interaction of the adsorbate molecules-adsorbate molecules. The magnitude of adsorption energy is lower than 40, which confirms the predominance of the physical adsorption process [30]. The total amount of xylene adsorbed at the saturation state (Q_{sat} mg g^{-1}) can be calculated as follows:

$$Q_{sat} = nN_m(1+N) \tag{18}$$

The calculated Q_{sat} for xylene adsorbed onto activated charcoal is presented in Table 4. This calculated value represents the high potential of the prepared activated charcoal toward xylene removal from aqueous solution. The parameters of the MLM-S isotherm at various temperatures are given in Table 3 and indicate that the number of xylene molecules adsorbed onto one adsorption site (*n*) increases with the rising of the temperature. This trend could be related to an increase in the ions or molecules collision with temperature increasing [38].

Table 3. The constant parameters of Langmuir, Hill, Double Layer, and Multilayer with saturation model

Multilayer with Saturation model

Parameters	*n*	N_m	c_1	c_2	*N*	R^2
25 °C	0.403	10.013	2.919	11.919	4.09	0.999476
35 °C	0.518	8.53	1.353	9.3857	4.131	0.998304
45 °C	0.631	7.0197	0.5993	1.9954	4.325	0.999283

Double Layer Model

Parameters	*n*	N_m	c_1	c_2	R^2
25 °C	1.02	27.93	3.223	9.29	0.988236
35 °C	0.849	22.775	2.1659	1.7853	0.982805
45 °C	0.862	35.112	0.6427	4.033	0.988876

Hill Model

Parameters	*n*	*q*	$c_{1/2}$	R^2
25 °C	0.702	1.846	2.266	0.972
35 °C	1.108	42.212	2.083	0.971
45 °C	0.711	49.814	1.891	0.978

Langmuir Model

Parameters	q_{max}	K_L	R^2
25 °C	46.948	0.173	0.94
35 °C	49.751	2.895	0.70
45 °C	58.139	3.230	0.69

Table 4. The amount of xylene adsorbed at saturation state and the adsorption energy

Temp.	Q_{sat} (mg/g	ε_1 (kJ/mol)	ε_2 (kJ/mol)
25 ºC	20.539	5.654	2.168
35 ºC	22.671	7.935	2.975
45 ºC	23.586	10.516	7.336

3.2.3. Mechanism of xylene adsorption

The adsorption potential of the prepared activated charcoal can be explained as a result of its functional groups and porosity. The kinetics analysis shows that pore diffusion is the important step for xylene adsorption onto activated charcoal. Also, there are some acidic and basic functional groups on its surface. These surface groups have oxygen (such as carboxylic acid, lactonic, carbonyl, and phenolic groups) that can adsorb the xylene via physical interactions such as the van der Waals interaction and/or hydrogen bonding.

4. Conclusions

A porous adsorbent was synthesized by chemically activating palm kernel biomass. The produced activated charcoal was used to remove xylene from aqueous solution. A mathematical model was presented to predict the adsorption performance at different conditions. The mass transfer parameters that included surface and pore diffusion coefficients as well as external mass transfer parameter were calculated via the model. The sensitivity analysis indicated that the external and pore diffusions steps were very important and rate-controlling. The equilibrium analysis indicated that the statistical physical modelling was a suitable approach to describe the microscopic characteristics of xylene adsorption onto activated charcoal. The chemical and physical parameters involved in the adsorption were determined by this method. The results showed that xylene adsorption onto this adsorbent was a multi-adsorption site (anchorage) process, and the geometry of xylene ions adsorbed onto adsorbent surface was parallel. The values of the adsorption energies implied that the xylene adsorption had an endothermic nature. Also, the results indicated that xylene adsorption onto activated charcoal was a multilayer and physical base process. Based on the equilibrium analysis, the synthesized activated charcoal was able to attract 23.58 mg of xylene per 1 g of charcoal. These results confirm that the synthesized activated charcoal has a favourable adsorption potential for xylene separation from dilute solutions.

References

[1] Aivalioti, M., Pothoulaki, D., Papoulias, P., Gidarakos, E. (2012). Removal of BTEX, MTBE and TAME from aqueous solutions by adsorption onto raw and thermally treated lignite. *Journal of hazardous materials*, *207*, 136-146.

[2] World Health Organization. (2004). *Guidelines for drinking-water quality: recommendations* (Vol. 1). World Health Organization.

[3] Saha, D., Mirando, N., Levchenko, A. (2018). Liquid and vapor phase adsorption of BTX in lignin derived activated carbon: Equilibrium and kinetics study. *Journal of cleaner production*, *182*, 372-378.

[4] Sangkhun, W., Laokiat, L., Tanboonchuy, V., Khamdahsag, P., Grisdanurak, N. (2012).

Photocatalytic degradation of BTEX using W-doped TiO2 immobilized on fiberglass cloth under visible light. *Superlattices and microstructures*, *52*(4), 632-642.

[5] Mazzeo, D. E. C., Levy, C. E., de Angelis, D. D. F., Marin-Morales, M. A. (2010). BTEX biodegradation by bacteria from effluents of petroleum refinery. *Science of the total environment*, *408*(20), 4334-4340.

[6] Mathur, A. K., Balomajumder, C. (2013). Biological treatment and modeling aspect of BTEX abatement process in a biofilter. *Bioresource technology*, *142*, 9-17

[7] Chovau, S., Dobrak, A., Figoli, A., Galiano, F., Simone, S., Drioli, E., Van der Bruggen, B. (2010). Pervaporation performance of unfilled and filled PDMS membranes and novel SBS membranes for the removal of toluene from diluted aqueous solutions. *Chemical engineering journal*, *159*(1-3), 37-46.

[8] Mehrabi, N., Soleimani, M., Yeganeh, M. M., Sharififard, H. (2015). Parameter optimization for nitrate removal from water using activated carbon and composite of activated carbon and Fe_2O_3 nanoparticles. *RSC advances*, *5*(64), 51470-51482.

[9] Sharififard, H., Pepe, F., Soleimani, M., Aprea, P., Caputo, D. (2016). Iron-activated carbon nanocomposite: synthesis, characterization and application for lead removal from aqueous solution. *RSC advances*, *6*(49), 42845-42853.

[10] Sharififard, H., Soleimani, M., Ashtiani, F. Z. (2014). Evaluation of chitosan flakes as adsorbent for palladium and platinum recovery from binary dilute solutions. *International journal of global warming*, *6*(2-3), 303-314.

[11] Heydari, S., Sharififard, H., Nabavinia, M., Kiani, H., Parvizi, M. (2013). Adsorption of chromium ions from aqueous solution by carbon adsorbent. *International journal of environmental, chemical, ecological, geological and geophysical engineering*, *7*(12), 649-652.

[12] Bansal, R. C., Goyal, M. (2005). *Activated carbon adsorption*. CRC press.

[13] Çeçen, F., Aktas, Ö. (2011). *Activated carbon for water and wastewater treatment: Integration of adsorption and biological treatment*. John Wiley and Sons.

[14] Bandosz, T. J. (2006). *Activated carbon surfaces in environmental remediation* (Vol. 7). Elsevier.

[15] Niazi, L., Lashanizadegan, A., Sharififard, H. (2018). Chestnut oak shells activated carbon: Preparation, characterization and application for Cr (VI) removal from dilute aqueous solutions. *Journal of cleaner production*, *185*, 554-561.

[16] Shahraki, Z. H., Sharififard, H., Lashanizadegan, A. Grape stalks biomass as raw material for activated carbon production: Synthesis, characterization and adsorption ability. Materials research express, 5(5), doi.org/10.1088/2053-1591/aac1cd.

[17] Demiral, H., Güngör, C. (2016). Adsorption of copper (II) from aqueous solutions on activated carbon prepared from grape bagasse. *Journal of cleaner production*, *124*, 103-113.

[18] Al Bahri, M., Calvo, L., Gilarranz, M. A., Rodriguez, J. J. (2016). Diuron multilayer adsorption on activated carbon from CO2 activation of grape seeds. *Chemical engineering communications*, *203*(1), 103-113.

[19] Altintig, E., Kirkil, S. (2016). Preparation and properties of Ag-coated activated carbon nanocomposites produced from wild chestnut shell by $ZnCl_2$ activation. *Journal of the Taiwan institute of chemical engineers*, *63*, 180-188.

[20] Nowicki, P., Kazmierczak, J., Pietrzak, R. (2015). Comparison of physicochemical and sorption properties of activated carbons prepared by physical and chemical activation of cherry stones. *Powder technology*, *269*, 312-319.

[21] Chen, Y., Zhai, S. R., Liu, N., Song, Y., An, Q. D., Song, X. W. (2013). Dye removal of activated carbons prepared from NaOH-pretreated rice husks by low-temperature solution-processed carbonization and H_3PO_4 activation. *Bioresource technology*, *144*, 401-409.

[22] Lin, L., Zhai, S. R., Xiao, Z. Y., Song, Y., An, Q. D., Song, X. W. (2013). Dye adsorption of mesoporous activated carbons produced from NaOH-pretreated rice husks. *Bioresource technology*, *136*, 437-443.

[23] American Society for Testing and Materials. (1991). Standard Test Methods for Moisture in Activated Charcoal, ASTM Committee on Standards, Philadelphia.

[24] American Society for Testing and Materials. (2000). Designation D4607-94, ASTM Committee on Standards, Philadelphia.

[25] Kaghazchi, T., Kolur, N. A., Soleimani, M. (2010). Licorice residue and Pistachio-nut shell mixture: A promising precursor for activated carbon. *Journal of industrial and engineering chemistry*, *16*(3), 368-374.

[26] Laksaci, H., Khelifi, A., Trari, M., Addoun, A. (2017). Synthesis and characterization of microporous activated carbon from coffee grounds using potassium hydroxides. *Journal of cleaner production*, *147*, 254-262.

[27] Sharififard, H., Soleimani, M., Zokaee Ashtiani, F. (2016). Application of nanoscale iron oxide-hydroxide-impregnated activated carbon (Fe-AC) as an adsorbent for vanadium recovery from aqueous solutions. *Desalination and water treatment*, *57*(33), 15714-15723.

[28] Badruzzaman, M., Westerhoff, P., Knappe, D. R. (2004). Intraparticle diffusion and adsorption of arsenate onto granular ferric hydroxide (GFH). *Water research*, *38*(18), 4002-4012.

[29] Sharififard, H., Soleimani, M. (2017). Modeling and experimental study of vanadium adsorption by iron-

nanoparticle-impregnated activated carbon.*Research on chemical intermediates*, *43*(4), 2501-2516.

[30] Sellaoui, L., Guedidi, H., Knani, S., Reinert, L., Duclaux, L., Lamine, A. B. (2015). Application of statistical physics formalism to the modeling of adsorption isotherms of ibuprofen on activated carbon. *Fluid phase equilibria*, *387*, 103-110

[31] Dotto, G. L., Pinto, L. A. A., Hachicha, M. A., Knani, S. (2015). New physicochemical interpretations for the adsorption of food dyes on chitosan films using statistical physics treatment. *Food chemistry*, *171*, 1-7.

[32] Coquelet, C., Valtz, A., Richon, D. (2008). Solubility of ethylbenzene and xylene in pure water and aqueous alkanolamine solutions. *The journal of chemical thermodynamics*, *40*(6), 942-948.

[33] Sellaoui, L., Mechi, N., Lima, É. C., Dotto, G. L., Lamine, A. B. (2017). Adsorption of diclofenac and nimesulide on activated carbon: statistical physics modeling and effect of adsorbate size. *Journal of physics and chemistry of solids*, *109*, 117-123.

[34] Nunell, G. V., Fernández, M. E., Bonelli, P. R., Cukierman, A. L. (2012). Conversion of biomass from an invasive species into activated carbons for removal of nitrate from wastewater. *Biomass and bioenergy*, *44*, 87-95.

[35] da Silva Lacerda, V., López-Sotelo, J. B., Correa-Guimarães, A., Hernández-Navarro, S., Sánchez-Báscones, M., Navas-Gracia, L. M., Martín-Gil, J. (2015). Rhodamine B removal with activated carbons obtained from lignocellulosic waste. *Journal of environmental management*, *155*, 67-76

[36] Lim, W. C., Srinivasakannan, C., Balasubramanian, N. (2010). Activation of palm shells by phosphoric acid impregnation for high yielding activated carbon. *Journal of analytical and applied pyrolysis*, *88*(2), 181-186.

[37] Knani, S., Aouaini, F., Bahloul, N., Khalfaoui, M., Hachicha, M. A., Lamine, A. B., Kechaou, N. (2014). Modeling of adsorption isotherms of water vapor on Tunisian olive leaves using statistical mechanical formulation. *Physica A: Statistical mechanics and its applications*, *400*, 57-70.

[38] Khalfaoui, M., Baouab, M. H. V., Gauthier, R., Lamine, A. B. (2006). Acid dye adsorption onto cationized polyamide fibres. Modeling and consequent interpretations of model parameter behaviours. *Journal of colloid and interface science*, *296*(2), 419-427.